Макрогетероциклы
http://macroheterocycles.isuct.ru

DOI: 10.6060/mhc181005l

π−Extended BODIPY Analogues: Synthesis, Electronic Structure, Potential Utility for *in vivo* Imaging Applications and Cytotoxicity

Xu Liang,[a,c@1] He Luo,[a] Yaquan Lan,[a] Weihua Zhu,[a] John Mack,[b@2] Zweli Hlatshwayo,[b] Tebello Nyokong,[b] and Qiuyun Chen[a@3]

[a]*School of Chemistry and Chemical Engineering, Jiangsu University, 212013 Zhenjiang, P. R. China*
[b]*Department of Chemistry, Rhodes University, 6140 Grahamstown, South Africa*
[c]*State Key Laboratory of Coordination Chemistry, Nanjing University, 212013 Nanjing, P. R. China*
[@1]*E-mail: liangxu@ujs.edu.cn*
[@2]*E-mail: j.mack@ru.ac.za*
[@3]*E-mail: chenqy@ujs.edu.cn*

*A series of 3,5-distyryl and meso-morpholino/hydroquinoline BODIPY dyes have been synthesized and characterized. The electronic structure was investigated by optical spectroscopy, electrochemistry and TD-DFT calculations. In addition, they fluoresce in the biological window and are hence potentially suitable for use as cellular imaging agents. The meso-1,2,3,4-isoquinoline substituted BODIPYs **3c-d** interact strongly with DNA and this enhances their ability to act as bioimaging agents. In contrast, the meso-morpholine substituted BODIPYs **3a-b** were found to have higher cell toxicity.*

Keywords: BODIPY, electronic structure, cellular imaging, cell toxicity.

Аналоги BODIPY с расширенной π−системой: Синтез, электронная структура, потенциальное применение для визуализации *in vivo* и цитотоксичность

К. Лианг,[a,c@1] Х. Луо,[a] Я. Лан,[a] В. Жу,[a] Дж. Мак,[b@2] З. Хлатшвайо,[b] Т. Ниоконг,[b] К. Чен[a@3]

[a]*Школа химии и химической инженерии, Университет Цзянсу, 212013 Чжэньцзян, Китай*
[b]*Кафедра химии, Университет Родса, 6140 Грэхэмстаун, ЮАР*
[c]*Государственная ключевая лаборатория координационной химии, Нанкинский университет, 212013 Нанкин, Китай*
[@1]*E-mail: liangxu@ujs.edu.cn*
[@2]*E-mail: j.mack@ru.ac.za*
[@3]*E-mail: chenqy@ujs.edu.cn*

*В данной работе синтезирована и охарактеризована серия 3,5-дистирил и мезо-морфолино/оксихинолин красителей BODIPY, методами оптической спектроскопии, электрохимии и TD-DFT расчетами исследована их электронная структура. Флуоресцентные свойства полученных соединений позволяют рассматривать их в качестве перспективных агентов визуализации клеток. мезо-1,2,3,4-Изохинолинзамещенные BODIPY **3c-d** сильно взаимодействуют с молекулами ДНК, что привлекательно с точки зрения использования их в биоимиджинге. мезо-Морфолинзамещенные BODIPY **3a-b** обладают более высокой клеточной токсичностью.*

Keywords: BODIPY, электронная структура, клеточная визуализация, клеточная токсичность.

Introduction

Ideal molecules used for bioimaging applications should absorb and emit strongly in the red/near-infrared (NIR) spectral region and have narrow spectra bands, large Stokes shifts, long excited-state lifetimes, excellent photostability, and low biotoxicity. Research in this area has focused on chromophores, such as porphyrins, corroles and phthalocyanines.[1-3] More recently, there has been growing interest in the use of BODIPY (difluoroboradipyrromethenes) dyes in this context,[4-8] since they have high fluorescence quantum yields and intense absorption and fluorescence bands. In addition, the BODIPY chromophores could be facially modified through an extension of the π-conjugation system so that the fluorescence emission bands lie at the red end of the visible region or in the NIR in the optical window for biological tissues (650–1000 nm), making them potentially suitable for use as fluorescence cellular imaging agents.[9] Thus, there is currently considerable interest in the design and synthesis of novel BODIPY dyes with intense absorption and emission bands in this spectral region. In this study, styryl groups are introduced as substituents at the 3,5-positions on the pyrrole moieties through Knoevenagel condensation reactions (Scheme 1), since this is known to result in a large red shift of the main spectral bands into biological window. Moreover, morpholino and hydroquinoline and their derivative were widely used in organic and biological systems. Along with *meso*-phenyl substituents that enhance the solubility of the dyes in aqueous solution and their DNA binding properties. The suitability of the dyes for use as bioimaging agents is investigated in HepG-2 cells along were studied for antitumor activity *in vitro*.

Experimental

General

All reagents and solvents were of reagent grade quality and were used as received unless noted otherwise. ^{1}H and ^{19}F NMR spectra were recorded on a Bruker AVANCE 400 spectrometer (400.03 MHz). Residual solvent peaks were used to provide internal references for the ^{1}H NMR spectra (7.26 ppm for $CDCl_3$, and 5.32 ppm for CD_2Cl_2). FT-IR spectra were measured with a Nicolet Nexus 470 FT-IR spectrophotometer over the 4000–400 cm^{-1} energy range. Fluorescence measurements were performed on a CARY Eclipse spectrofluorometer (Varian, USA) in 1.0 cm quartz cells (λ_{ex}=460 nm, slit width=5 nm). Electrospray ionization mass spectrometry (ESI-MS) data were determined on a Finnigan LCQ mass spectrograph. The UV and visible regions of the electronic absorption spectra were recorded with an HP 8453A diode array spectrophotometer. A glassy carbon disk, a platinum wire and an Ag/AgCl electrode were used as the working, counter and reference electrodes, respectively, during electrochemical measurements with a Chi-730D electrochemical working station at room temperature. An inert nitrogen atmosphere was introduced during all electrochemical measurements. BODIPY **3b**-labelled HeLa cells were plated in a 24-well plate at a density of 2.4×10^4 cells mL^{-1}. After incubating for 24 h with the complexes, the cells were stained with DAPI, and nuclei change was visualized under a fluorescence microscope (Nikon TE2000 inverted microscope).

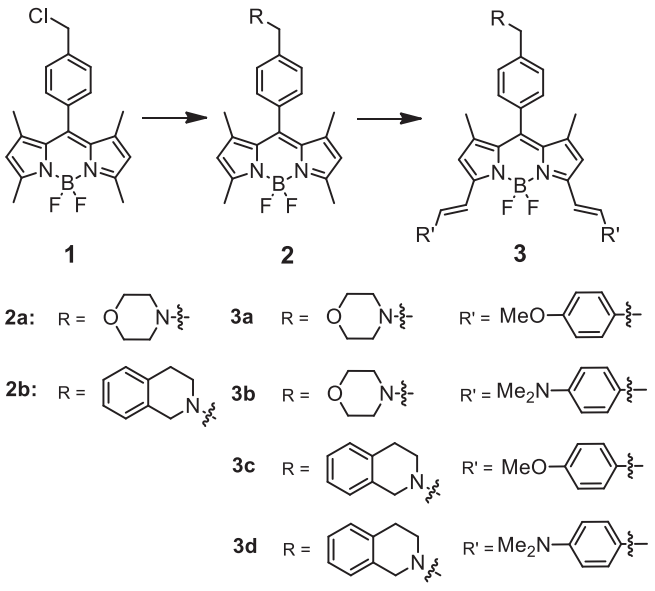

Scheme 1. The synthesis and molecular structures of **2a-b** and **3a-d**.

Computational Methods

The Gaussian 09 software package[10] was used to carry out DFT geometry optimizations for a *meso*-phenyltetramethylBODIPY model compound (BDY), **2a-b** and **3a-d** by using the B3LYP functional with 6-31G(d) basis sets. TD-DFT calculations were carried out by using CAM-B3LYP functional, which includes a long-range correction of the exchange potential, since this provides more accurate results for complexes that have excited states with significant intramolecular charge transfer character.[11,12]

Cytotoxicity Testing

Cytotoxicity assays were measured with HepG-2 cells in normal culture conditions. HepG-2 cells were seeded at a density of 4×10^{-4} cells mL^{-1} into sterile 96-well plates. **3a-d** were added in DMSO and diluted with culture media. After 24 h, compounds were added into the cultured HepG-2 cells for a further 24 h. Cell viability was determined by the 3-[4,5-dimethylthiazol-2-yl]-2,5-diphenyltetrazolium bromide (MTT) assay by measuring the absorbance at 570 nm. Each test was performed in triplicate.

Synthesis

*4-(4-(5,5-Difluoro-1,3,7,9-tetramethyl-5H-4λ,5λ-dipyrrolo[1,2-c:2',1'-f][1,3,2]-diazaborinin-10-yl)benzyl) morpholine (**2a**).* A 15 mL THF solution containing BODIPY **1** (372.1 mg, 1.0 mmol), morpholine (173.3 mg, 2.0 mmol) and 0.5 mL triethylamine was stirred at 65 °C for 6 h, and the p*H* was strictly controlled to lie between p*H*=7–8. After removal of the solvent, the residue was dissolved in 20 mL CH_2Cl_2, washed three times with brine and dried over Na_2SO_4. The target compound was obtained by silica gel column chromatography (eluent: petroleum ether:ethyl acetate=5:1; v:v) as a red solid in 71.2 % yield (301.5 mg). Elemental analysis (%): Found: C 68.00, H 6.50, N 10.00, O 3.80, B 2.61, F 9.11. Calcd (%) for $C_{24}H_{28}BF_2N_3O$: C 68.10, H 6.67, N 9.93, O 3.78, B 2.55, F 8.98. *m/z* (ESI-MS) 424.48 (Calcd for $C_{24}H_{28}BF_2N_3O$, $[M+H]^+$=424.23). IR (KBr) ν_{max} cm^{-1}: 2956, 2922, 2855, 2801, 1547, 1509, 1468, 1408, 1365, 1304, 1194, 1047, 980, 821, 754, 706. ^{1}H NMR (400 MHz, $CDCl_3$) δ_H ppm: 7.46–7.44 (d, *J*=8 Hz, 2H), 7.24–7.22 (d, *J*=8 Hz, 2H), 5.97 (s, 2H), 3.75–3.72 (t, *J*=6 Hz, 4H), 3.59 (s, 2H), 2.55 (s, 6H), 2.46 (s, 4H), 1.37 (s, 6H).

*10-(4-((3,4-Dihydroisoquinolin-2(1H)-yl)methyl)phenyl)-5,5-difluoro-1,3,7,9-tetramethyl-5H-4λ,5λ-dipyrrolo[1,2-c:2',1'-f][1,3,2]diazaborinine (**2b**).* A THF solution (15 mL) containing **1** (372.1 mg, 1.0 mmol), 1,2,3,4-isoquinoline (160 mg, 1.2 mmol, 1.2 eq), K_2CO_3 (166.0 mg, 1.2 mmol), KI (34.2 mg, 0.2 mmol) and a catalytic amount of 18-crown-6 ether was stirred at 60 °C for 5 h under N_2. After removal of the solvent, the residue was dissolved in 20 mL CH_2Cl_2, washed three times with brine and dried over Na_2SO_4. The target compound was obtained by silica gel column chromatography (eluent: petroleum oil:ethyl acetate = 10:1; v:v) as a red solid in 73.0 % yield (342.5 mg). Elemental analysis (%): Found: C 74.11, H 6.55, N 8.83, B 2.38, F 8.15. Calcd (%) for $C_{29}H_{30}BF_2N_3$: C 74.21, H 6.44, N 8.95, B 2.30, F 8.09. *m/z* (ESI-MS) 470.54 (Calcd for $C_{29}H_{30}BF_2N_3$ $[M+H]^+$ = 470.39). IR (KBr) ν_{max} cm^{-1}: 2919, 2851, 1538, 1463, 1409, 1357, 1304, 1254, 1187, 1154, 1070, 972, 806, 761, 693. ^1H NMR (400 MHz, $CDCl_3$) δ_H ppm: 7.55–7.53 (d, *J*=8 Hz, 2H), 7.26–7.25 (d, *J*=4 Hz, 2H), 7.14 (m, 3H), 6.98–6.96 (d, *J*=8Hz, 1H), 5.99 (s, 2H), 3.80 (s, 2H), 3.65 (s, 2H), 2.96–2.93 (t, *J*=6 Hz, 2H), 2.82–2.79 (t, *J*=6 Hz, 2H), 2.56 (s, 6H), 1.41 (s, 6H).

*4-(4-(5,5-Difluoro-3,7-(4-methoxystyryl)-1,9-dimethyl-5H-4λ,5λ-dipyrrolo[1,2-c:2',1'-f][1,3,2]diazaborinin-10-yl)benzyl)morpholine (**3a**).* **2a** (234.5 mg, 0.5 mmol) and *p*-methoxylbenzaldehyde (170.5 mg, 1.3 mmol) were dissolved in 15 mL toluene, and 4-methylphenylsulfonic acid and piperidine (8.7 mg, 0.1 mmol) were slowly added. The mixture was refluxed at 120 °C under N_2 for about 8 h. After removal of the solvent, pure target compound was obtained by silica gel column chromatography (eluent: petroleum oil:ethyl acetate=3:1; v:v) as a blue purple solid in 36.4 % yield (102.4 mg). Elemental analysis (%): Found: C 72.70, H 6.20, N 6.20, O 7.36, B 1.61, F 5.71. Calcd (%) for $C_{40}H_{40}BF_2N_3O_3$: C 72.84, H 6.11, N 6.37, O 7.28, B 1.64, F 5.76. *m/z* (ESI-MS) 660.52 (Calcd for $C_{40}H_{40}BF_2N_3O_3$ $[M+H]^+$=660.58). IR (KBr) ν_{max} cm^{-1}: 3420, 2933, 2842, 1603, 1540, 1484, 1377, 1301, 1247, 1201, 1168, 1107, 1021, 990, 865, 821, 765, 719. ^1H NMR (400 MHz, $CDCl_3$) δ_H ppm: 7.63 (s, 1H), 7.59–7.57 (m, 5H), 7.47–7.45 (d, *J*=8 Hz, 2H), 7.29–7.26 (m, 2H), 7.23 (s, 1H), 7.19 (s, 1H), 6.94–6.92 (d, *J*=8 Hz, 4H), 6.61 (s, 2H), 3.85 (s, 6H), 3.75 (m, 4H), 3.61 (s, 2H), 2.48 (m, 4H), 1.38 (s, 6H).

*4,4'-((5,5-Difluoro-1,9-dimethyl-10-(4-morpholinomethyl)phenyl)-5H-4λ,5λ-dipyrrolo[1,2-c:2',1'-f][1,3,2]diazaborinin-3,7-diyl)(ethene-2,1-diyl)-N,N-dimethylaniline (**3b**).* A synthetic procedure similar to that of **3a** was followed with *N*,*N*-dimethylaminophenylbenzaldehyde used instead. The target compound was obtained as a deep blue solid in 42.1 % yield (141.2 mg). Elemental analysis (%): Found: C 73.70, H 6.70, N 10.30, O 2.26, B 1.51, F 5.46. Calcd (%) for $C_{42}H_{48}BF_2N_5O$: C 73.57, H 6.76, N 10.21, O 2.33, B 1.58, F 5.54. *m/z* (ESI-MS) 686.74 (Calcd for $C_{40}H_{40}BF_2N_3O_3$ $[M+H]^+$ = 686.67). IR (KBr) ν_{max} cm^{-1}: 3420, 2918, 2851, 2806, 1596, 1531, 1481, 1362, 1293, 1160, 1107, 1064, 987, 949, 858, 808, 764. ^1H NMR (400 MHz, $CDCl_3$) δ_H ppm: 7.58 (s, 1H), 7.55–7.52 (m, 5H), 7.45–7.43 (d, *J*=8 Hz, 2H), 7.29–7.27 (d, *J*=8 Hz, 2H), 7.21 (s, 1H), 7.17 (s, 1H), 6.72–6.70 (d, *J*=8 Hz, 4H), 6.59 (s, 2H), 3.76–3.74 (t, *J*=4 Hz, 4H), 3.60 (s, 2H), 3.03 (s, 12H), 2.47 (m, 4H), 1.42 (s, 6H).

*10-(4((3,4-Dihydroisoquinolin-2(1H)-yl)methyl)phenyl)-5,5-difluoro-3,7-(4-methoxystyryl)-1,9-dimethyl-5H-4λ,5λ-dipyrrolo[1,2-c:2',1'-f][1,3,2]diazaborinine (**3c**).* A synthetic procedure similar to that of **3a** was followed, but precursor **2b** was used instead. The target compound was successfully obtained as a purple solid in 43.4 % yield (153.0 mg). Elemental analysis (%): Found: C 76.70, H 6.10, N 5.90, O 4.46, B 1.46, F 5.34. Calcd (%) for $C_{45}H_{42}BF_2N_3O_2$: C 76.59, H 6.00, N 5.95, O 4.53, B 1.53, F 5.38. *m/z* (ESI-MS) 706.54 (Calcd for $C_{45}H_{42}BF_2N_3O_2$ $[M+H]^+$=706.66). IR (KBr) ν_{max} cm^{-1}: 3412, 3069, 3007, 2956, 2926, 2843, 1606, 1545, 1485, 1357, 1304, 1198, 1143, 979, 829, 761, 708. ^1H NMR (400 MHz, $CDCl_3$) δ_H ppm: 7.64 (s, 1H), 7.60–7.58 (d, *J*=8 Hz, 5H), 7.54–7.52 (d, *J*=8 Hz, 2H), 7.31–7.29 (d, *J* = 8 Hz, 2H), 7.24 (s, 1H), 7.20 (s, 1H), 7.14–7.12 (m, 3H), 6.99–6.97 (d, *J*=8 Hz, 1H), 6.95–6.93 (d, *J*=8 Hz, 4H), 6.62 (s, 2H), 3.86 (s, 6H), 3.80 (s, 2H), 3.65 (s, 2H), 2.96–2.93 (t, *J*=6 Hz, 2H), 2.81–2.78 (t, *J*=6 Hz, 2H), 1.47 (s, 6H).

*4,4'-(10-(4((3,4-Dihydroisoquinolin-2(1H)-yl)methyl)phenyl)-5,5-difluoro-1,9-dimethyl-5H-4λ,5λ-dipyrrolo[1,2-c:2',1'-f][1,3,2]diazaborinine-3,7-diyl)(ethene-2,1-diyl)-N,N-dimethylaniline (**3d**).* A synthetic procedure similar to that of **3c** was followed with dimethylaminophenylbenzaldehyde used instead. The target compound was obtained in 9.4 % yield (142 mg). Elemental analysis: Found: C 77.10, H 6.67, N 9.50, B 1.46, F 5.10. Calcd (%) for $C_{47}H_{48}BF_2N_5$: C 77.15, H 6.61, N 9.57, B 1.48, F 5.19. *m/z* (ESI-MS) 732.53 (Calcd for $C_{37}H_{36}BF_2N_3O$) $[M+H]^+$=732.74). IR (KBr) ν_{max} cm^{-1}: 3025, 2922, 2848, 2801, 1594, 1527, 1479, 1362, 1294, 1252, 1161, 1151, 989, 950, 820, 761, 689. ^1H NMR (400 MHz, $CDCl_3$) δ_H ppm: 7.59 (s, 1H), 7.55–7.50 (m, 7H), 7.31–7.29 (d, *J*=8 Hz, 2H), 7.21 (s, 1H), 7.17 (s, 1H), 7.14–7.12 (m, 3H), 6.99–6.98 (d, *J*=4 Hz, 1H), 6.73–6.71 (d, *J*=8 Hz, 4H), 6.60 (s, 2H), 3.79 (s, 2H), 3.65 (s, 2H), 3.04 (s, 12H), 2.96–2.93 (t, *J*=6 Hz, 2H), 2.81–2.78 (t, *J*=6 Hz, 2H), 1.46 (s, 6H).

Results and Discussion

Synthesis

Novel *meso*-morpholine and *meso*-1,2,3,4-isoquinoline substituted BODIPYs (**2a** and **2b**) were prepared from BODIPY **1** by modifying the substituent on the *meso*-carbon (Scheme 1). The methyl group protons of **2a** and **2b** are sufficiently acidic to undergo Knoevenagel condensation reactions.[13,14] The introduction of styryl groups to form **3a-d** is one of the main strategies for shifting the main spectral bands into the biological window.[2]

Optical Spectroscopy

When a comparison is made with the main absorption band of the parent *meso*-phenyl-BODIPY complex at *ca*. 500 nm,[2] it becomes clear that only very minor spectral changes are observed for **2a** and **2b** (Figure 1), since the main absorption bands lie at 503 and 502 nm, respectively. This is the pattern that would be anticipated since the *meso*-substituent lies orthogonal to the BODIPY core for steric reasons. When further structural changes are made to form 3,5-distyrylBODIPYs **3a-d**, the extent of the observed red-shift is proportional to the electron donor ability of the styryl groups.[2] The main absorption bands of the *meso*-morpholine substituted **3a** and **3b** dyes lie at 642 and 693 nm (Figure 1), respectively, with a larger red shift observed when *p*-*N*,*N*-dimethylaminophenylstyryl groups are introduced. When the *meso*-substituent is changed to 1,2,3,4-isoquinoline, there are only minor spectral changes, since the main spectral bands of **3c** and **3d** lie at 641 and 696 nm (Figure 1). **2a-b**, and **3c-d** exhibit moderately intense fluorescence in THF at room temperature (Table 1), while those of morpholine substituted distyrylBODIPYs **3a** and **3b** are significantly lower. The fluorescence lifetimes values are consistent with those that have been reported previously for structurally similar 3,5-distyrylBODIPY dyes.[1,15] **3c**, which has methoxyphenylstyryl groups at the 3,5-positions and a *meso*-1,2,3,4-isoquinoline substituent, was found to have the highest

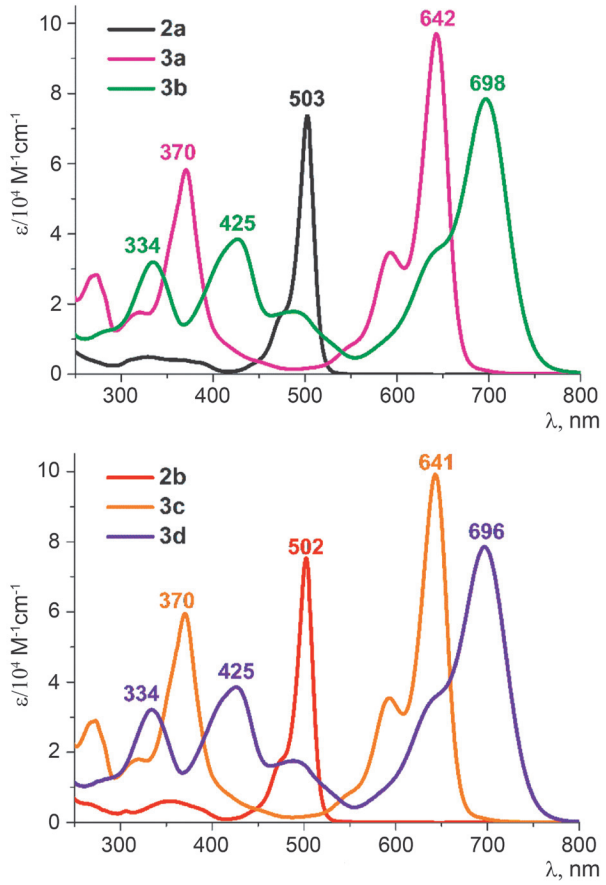

Figure 1. UV-visible absorption spectra of **2a-b** and **3a-d** in CH_2Cl_2.

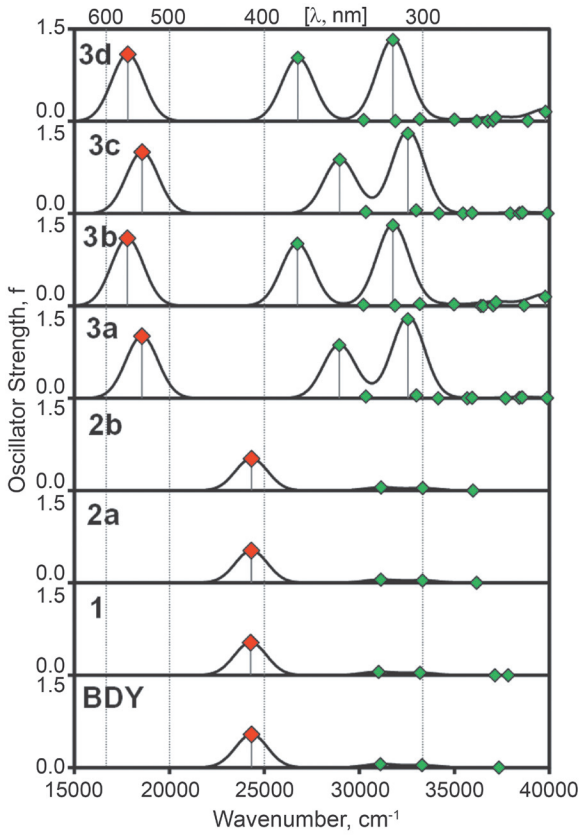

Figure 2. The calculated TD-DFT spectra of the B3LYP optimized geometries of the BDY model compound, **1**, **2a-b** and **3a-d** calculated at the CAM-B3LYP/6-31G(d) level of theory. The Chemcraft program was used to generate the simulated spectra by using bandwidths of 2000 cm^{-1}.

fluorescence quantum yield value. The most likely explanation for the increase relative to **3d** is that there is less intramolecular charge transfer character in the **S1** state than is the case when *p*-*N*,*N*-dimethylaminophenylstyryl groups are present. Larger Stokes shifts are observed for *meso*-1,2,3,4-isoquinoline substituted BODIPYs **3c-d** than for **3a-b**, due to changes in the structural dynamics in the excited states.

Theoretical Calculations

The observed spectral changes can be readily explained through a comparison with the results of TD-DFT calculations (Figure 2 and Table 2) at the CAM-B3LYP/6-31G(d) level of theory for B3LYP optimized geometries of the BDY model complex, **1**, **2a-b** and **3a-d**, since similar trends are observed in the energies of the main visible region spectral bands. In each case the HOMO → LUMO transition provides the predominant contribution to the lowest energy transition (Table 2). As has been reported previously,[2,15,16] the red shift that is caused by the introduction of electron donating styryl groups at the 3,5-positions of the BODIPY core is related to a relative destabilization of the HOMOs of **3a-d** (Figure 3), since the HOMO has larger MO coefficients at this position in the HOMO than in the LUMO resulting in a greater mesomeric interaction with the π-system of the styryl group that is co-planar with that of the BODIPY core. This results

Table 1. Spectroscopic data of **2a-b** and **3a-d**.

	λ_{abs} (max/nm)	λ_{em} (max/nm)	Stokes shift (cm^{-1})	$\varepsilon\times10^4$ ($L\cdot mol^{-1}\cdot cm^{-1}$)	τ (ns)	Φ_F (%)
2a	503	512	349	7.5	2.30±0.01	0.42±0.02
2b	503	512	349	8.3	2.29±0.01	0.48±0.02
3a	642	661	448	9.7	4.05±0.02	0.13±0.02
3b	641	656	357	9.9	4.03±0.01	0.08±0.01
3c	698	753	1046	7.8	2.26±0.01	0.41±0.02
3d	696	743	909	7.9	2.29±0.01	0.34±0.03

Table 2. Calculated wavelengths (λ), oscillator strengths (*f*) and the related wavefunctions of BDY, **2a-b** and **3a-d** at the CAM-B3LYP/6-31G(d) level of theory.

	State[a]	λ_{cal} (nm)[b]	λ_{exp} (nm)[c]	*f*[d]	Wavefunction[e]
neutral BODIPY compounds					
BDY	S_1	411	503[2]	0.54	H → L (97%)
1	S_1	412	–	0.53	H → L (97%)
2a	S_1	411	503	0.52	H → L (97%)
2b	S_1	411	502	0.52	H → L (97%)
3a	S_1	539	642	1.01	H → L (96%)
3b	S_1	562	698	1.10	H → L (95%)
3c	S_1	539	641	1.00	H → L (96%)
3d	S_1	562	696	1.09	H → L (95%)

[a]Excited state. [b]Calculated absorption wavelength in acetonitrile. [c]Experimental absorption wavelength in toluene. [d]Oscillator strength. [e]MOs involved in the transitions, H=HOMO, L=LUMO.

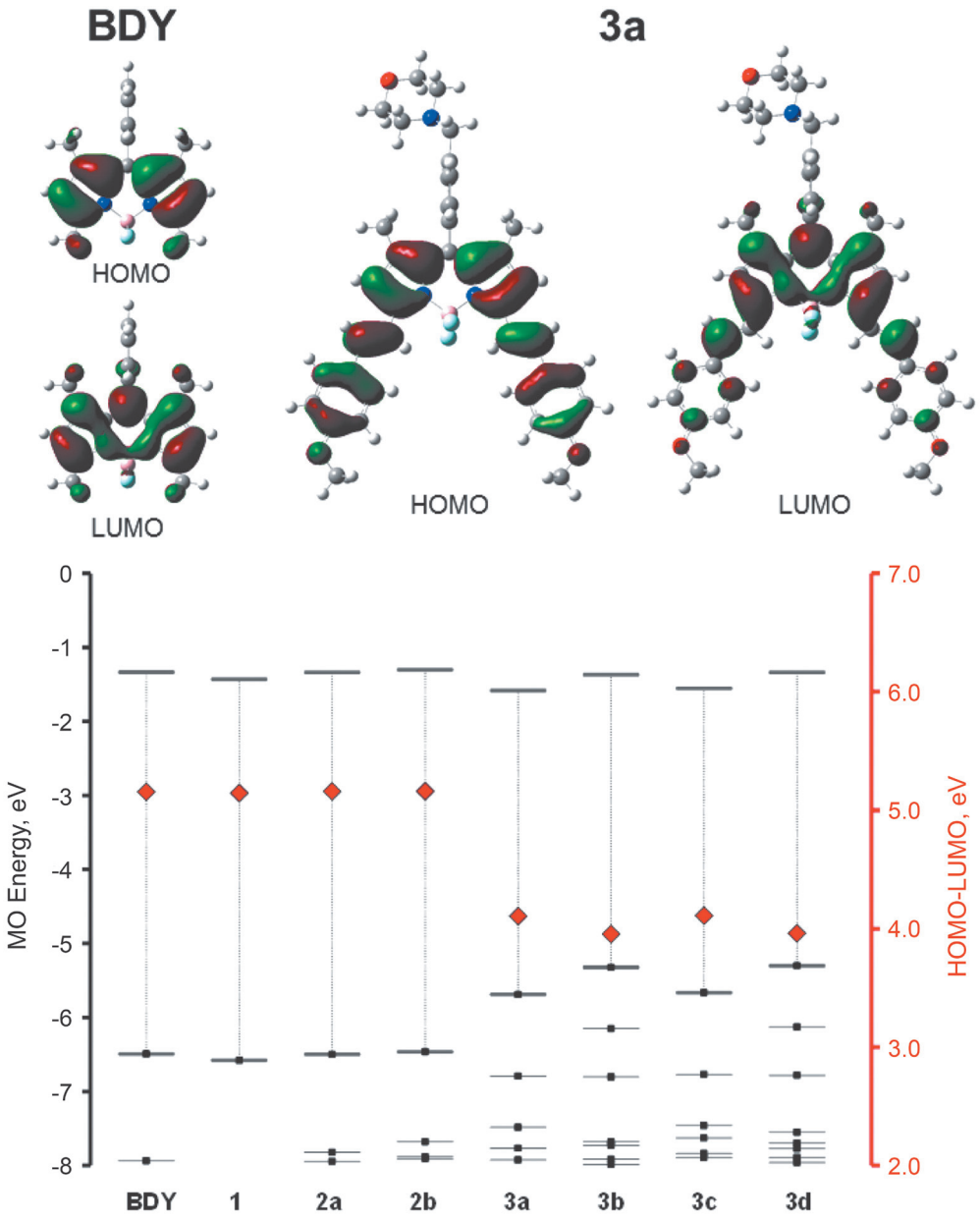

Figure 3. The MO energies of the BDY model compound, **1**, **2a-b** and **3a-d** calculated at the CAM-B3LYP/6-31G(d) level of theory (BOTTOM). The angular nodal patterns of the HOMO and LUMO of BDY and **3a** (TOP).

in a narrowing of the HOMO–LUMO gap and hence a large red shift of the main spectral bands.

Electrochemistry

In order to gain further insight into the electronic structures of **2a-b** and **3a-d**, cyclic and differential pulse voltammetry (CV and DPV) measurements were carried out in *o*-dichlorobenzene (*o*-DCB) containing 0.1 M tetra-*n*-butylammonium perchlorate (TBAP) as a supporting electrolyte (Figure 4), so that redox potential ($E_{1/2}$) values could be derived from both CV and DPV measurements. The electrochemical properties of **2a-b** are similar to those reported previously for other BODIPYs,[8] with a reduction step observed at –1.14 V. When electron-donating *p*-methoxyphenylstyryl and *p*-*N*,*N*-dimethylaminophenylstyryl groups are introduced at the 3,5-positions, two reversible processes are observed at –0.93 and –1.68 V for **3a** and –1.01 and –1.68 V for **3b**. 1,2,3,4-Isoquinoline substituted BODIPYs **3c-d** exhibit slight negative shifts in the reduction values at –1.00 and –1.76 V for **3c**, and –1.02 and –1.77 V for **3d**. The decrease in the first oxidation potentials of **3a-d** relative those of **2a-b** is consistent with what would be anticipated based on the destabilization of the HOMO in the theoretical calculations (Figure 3).

Interaction with ctDNA

BODIPYs **3a-b** are suitable for use as "turn-on" type fluorescence enhancing bioimaging agents, because the morpholine moieties enhance their lipophilicity. The complex formed between ethidium bromide (EB) and *ct*DNA (*ct*DNA-EB) has an intense fluorescence band at 602 nm

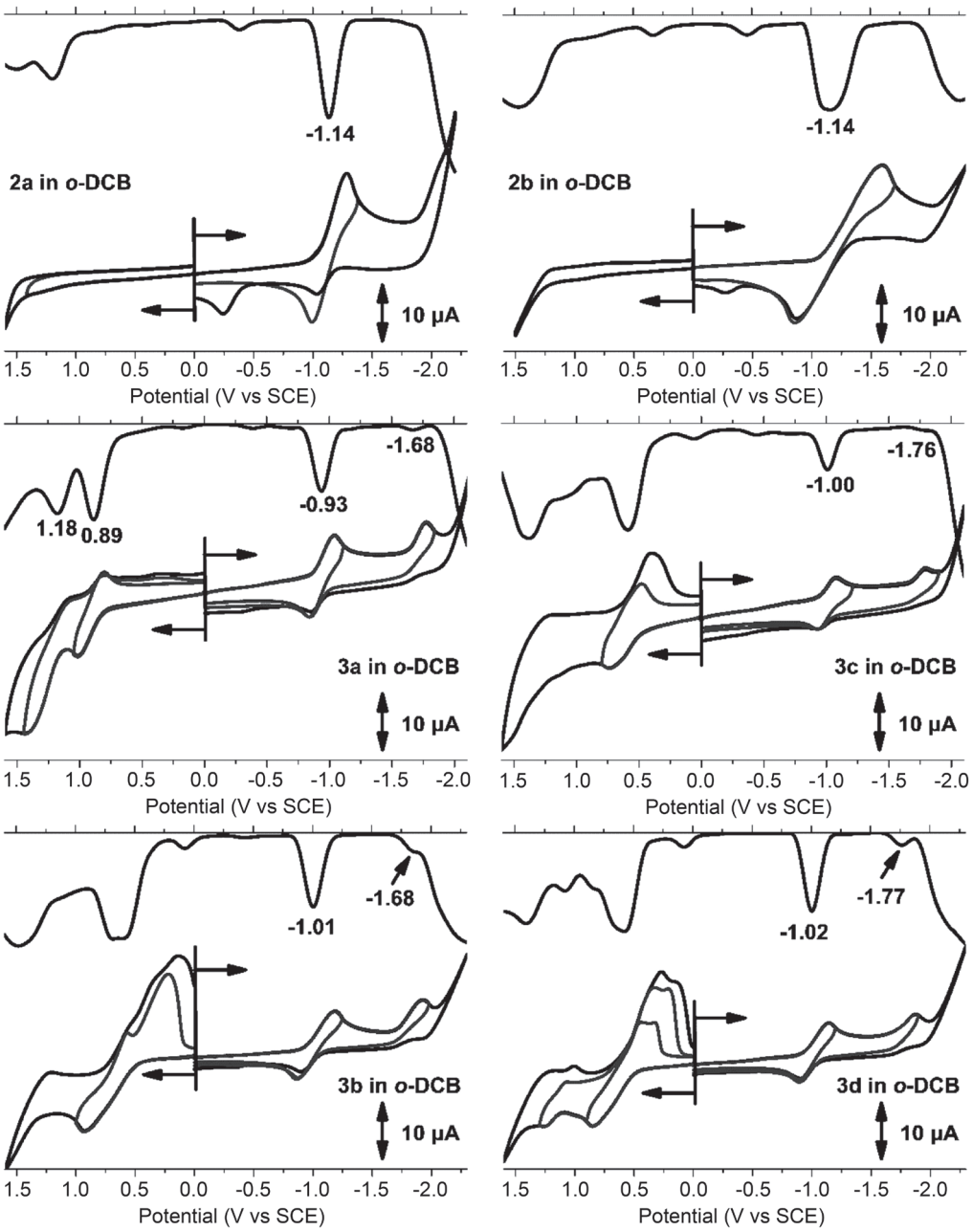

Figure 4. CV and DPV measurements of **2a-b** and **3a-d** in *o*-dichlorobenzene (*o*-DCB) containing 0.1 M TBAP.

(Figure 5). Upon addition of **3a-b**, the fluorescence intensity is significantly decreased due to the interaction between **3a-b** and *ct*DNA. According to the Stern-Volmer equation ($F_0/F=1+K_{sv}[Q]$), F_0 and F are the fluorescence intensities in the absence and presence of the quencher, respectively, K_{sv} is the linear Stern–Volmer quenching constant, and [Q] is the concentration of the quencher. **3a** and **3b** were found to have binding constants of 7130 and 7380 M^{-1}, respectively, on this basis.

Living Cell and Mitochondrial imaging

After treatment with HepG-2 cells for 4 h at 37 °C and washing with PBS solution, it can be clearly demonstrated that **3b** passed through the cell membrane and exhibited strong fluorescence inside the cell. Thus, BODIPY **3b** is suitable for use as a cell imaging agent. The targeting properties of the BODIPY complexes were analyzed by comparing the imaging effects of the **3b** complexes with those of Mito Tracker Green FM on mitochondria (Figure 6). The red fluorescence images overlap completely with the green fluorescence images of Mito Tracker Green FM, indicating that BODIPY **3b** can target mitochondria.

Cytotoxicity

3a-d were studied for antitumor activity *in vitro* by determining the inhibition of the growth of HepG-2 cells using MTT assays (Figure 7). The evaluation of the cytoxicity of **3a-d** at low concentrations (25 μM) suggests that the cell viability values of *meso*-morpholine substituted **3a-b** are lower than those for the *meso*-1,2,3,4-isoquinoline substituted **3c-d** compounds, since the 1,2,3,4-isoquinoline group readily reacts with oxygen and/or nitrogen containing compounds in the cell to enhance the cell toxicity. Upon increasing the concentration of **3a-d** in the same solutions to 50, 75 and 100 μM, the cell viability ratio steadily decreases as would be anticipated on this basis. **3a-b** have lower IC_{50} values for HepG-2 cell inhibition than **3c-d**.

Conclusions

A series of 3,5-distyryl BODIPY dyes have been prepared that fluoresce in the biological window and are hence potentially suitable for use as cellular imaging agents. The *meso*-1,2,3,4-isoquinoline-substituted BODIPYs **3a-d** interact strongly with DNA and this enhances their ability

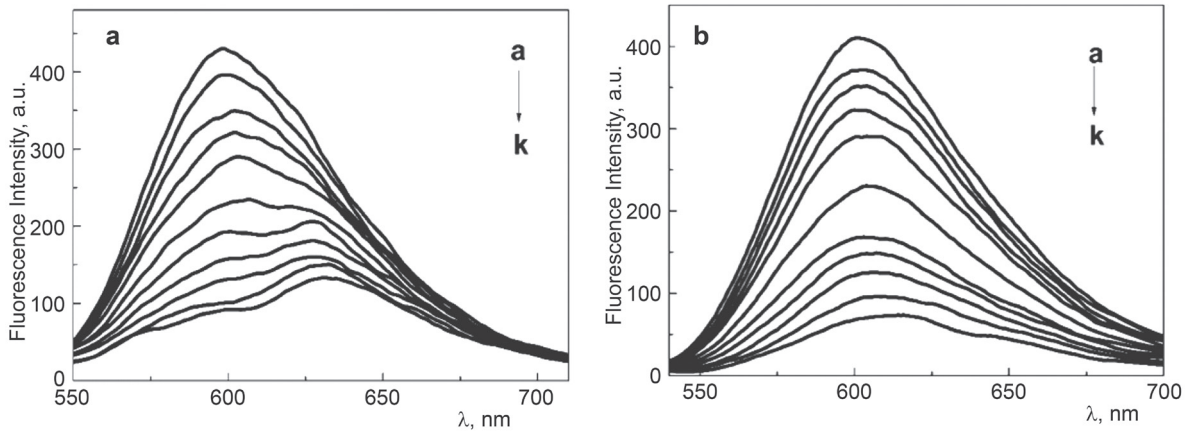

Figure 5. Fluorescence decay of *ct*DNA-EB upon addition of 0–200 μM (a–k) of **3a** (a) and **3b** (b). An excitation wavelength of 480 nm was used.

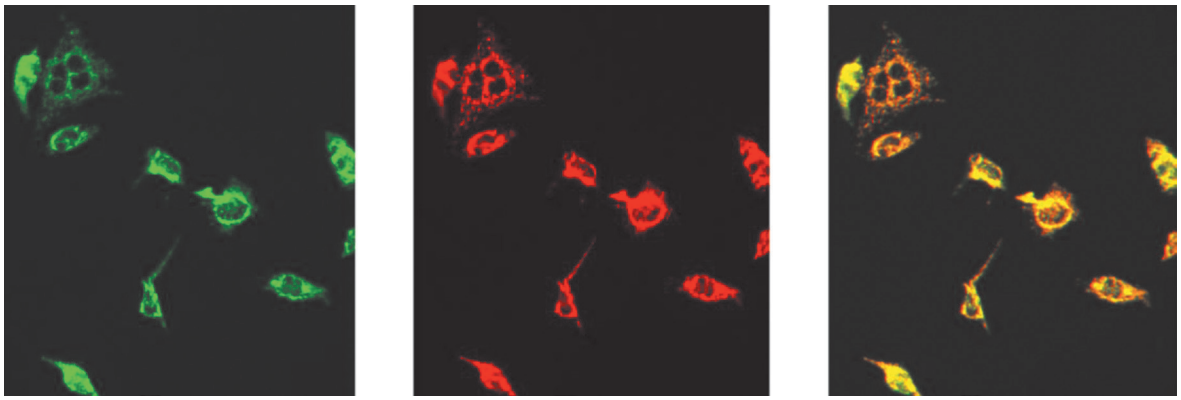

Figure 6. Fluorescence images of HepG-2 cells: Mito Tracker Green FM imaging (left); in the presence of **3b** (5 μM) image (middle); overlapped images (right).

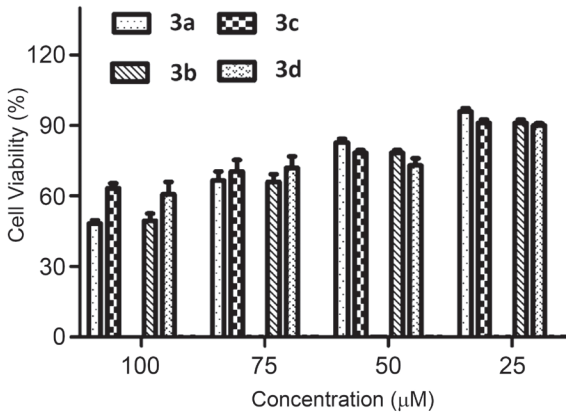

Figure 7. Inhibition activities of BODIPY derivatives **3a-d** on the proliferation of HepG-2 cells. HepG-2 cells in the absence of the compounds was used as the control.

to act as bioimaging agents. In contrast, the *meso*-morpholine-substituted BODIPYs **3a-d** were found to have slightly higher cell toxicity. Considering low toxic bio-inspired fluorescent molecules have a wide range of application, this study may enhance the understanding of the electronic structure of π-extended BODIPYs and their rational molecular design towards efficient biological applications.

Acknowledgements. This work was supported by the National Natural Science Foundation of China (project 21701058, 21571085), the Natural Science Foundation of Jiangsu province (project BK20160499), the State Key Laboratory of Coordination Chemistry (projects SKLCC1710 and SKLCC1817), the Key Laboratory of Functional Inorganic Material Chemistry (Heilongjiang University) of Ministry of Education, the China post-doc foundation (No. 2018M642183), the Lanzhou High Talent Innovation and Entrepreneurship Project (No. 2018-RC-105) and the Jiangsu University (project 17JDG035) to X. L. and Q.-Y. C., and a National Research Foundation (NRF) of South Africa through a CSUR grant from the NRF of South Africa to JM (uid: 93627). Photophysical measurements were made possible by the Laser Rental Pool Programme of the Council for Scientifc and Industrial Research (CSIR) of South Africa. Theoretical calculations were carried out at the Centre for High Performance Computing in Cape Town.

References

1. Wu P.J., Kuo S.Y., Huang Y.C., Chen C.P., Chan Y.H. *Anal. Chem.* **2014**, *86*, 4831.
2. Liang X., Mack J., Zheng L.M., Shen Z., Kobayashi N. *Inorg. Chem.* **2014**, *53*, 2797.
3. Liu J.J., Wang R., Wu S., Yuan B., Bao M.M., Li J.L., Dou Y.J., He Y., Yang K. *Nanotechnology* **2017**, *28*, 135601.
4. Loudet A., Burgess K. *Chem. Rev.* **2007**, *107*, 4891.
5. Boens N., Leen V., Dehaen W. *Chem. Soc. Rev.* **2012**, *41*, 1130.
6. Ulrich G., Ziessel R., Harriman A. *Angew. Chem. Int. Ed.* **2008**, *47*, 1184.
7. Lu H., Mack J., Yang Y., Shen Z. *Chem. Soc. Rev.* **2014**, *43*, 4778.
8. Nepomnyashchii A.B., Bard A.J. *Acc. Chem. Res.* **2012**, *45*, 1844.
9. Nu Y., Wu J. *Org. Bio. Chem.* **2014**, *12*, 3774.
10. Frisch M.J., Trucks G.W., Schlegel H.B., *et al. Gaussian 09., Revision A.02.* Gaussian., Inc., Wallingford C.T., **2016**.
11. Cai Z.L., Crossley M.J., Reimers J.R., Kobayashi R., Amos R.D. *J. Phys. Chem. B* **2006**, *110*, 15624.
12. Mack J., Wildervanck M., Nyokong T., *Turkish J. Chem.* **2014**, *38*, 1013.
13. Rurack K., Kollmannsberger M., Daub J. *Angew. Chem. Int. Ed.* **2001**, *40*, 385.
14. Wang S., Liu H., Mack J., Tian J., Zou B., Lu H., Li Z., Jiang J., Shen Z. *Chem. Commun.* **2015**, *51*, 13389.
15. Ngoy B.P., Molupe N., Harris J., Fomo G., Mack J., Nyokong T. *J. Porphyrins Phthalocyanines* **2017**, *21*, 431.
16. Gai L., Mack J., Lu H., Yamada H., Lai G., Li Z., Shen Z. *Chem. Eur. J.* **2014**, *20*, 1091.

Received 19.10.2018
Accepted 23.12.2018